Numerical Simulation of Critical Heat Flux of Flow Boiling in Oscillating Pipes

Nam-Kyu Ryu[a], Dae Seong Jo[b], Byeong-Jae Kim[a]*
[a]*Department of Mechanical Engineering, Chungnam National University, 99 Daehak-ro, Yuseong-gu, Daejeon*
[b]*Department of Mechanical Engineering, Kyungpook National University, 80 Daehakro, Bukgu, Daegu*
[*]*Corresponding author: bjkim@cnu.ac.kr*

1. Introduction

When the wall heat flux is high enough, a vapor blanket is formed on the wall causing rapid decrease of the heat transfer. This phenomenon is named departure from nucleate boiling (DNB), and the certain point that DNB appears is defined as critical heat flux(CHF). When DNB occurs, for the deterioration of heat transfer ability, wall temperature increases extremely, resulting in melt or destruction of the heated material. Hence it is essential to predict CHF to maintain the system safety.

To this day, CHF was mostly researched by experiments and empirical correlations. Because these correlations are based on experimental data, reasonable prediction with average derivation less than 25% are only able to be acquired under specific conditions. Furthermore, for such reason, these correlations are only available for certain geometries. Since most of these geometries have simple shape such as circular or rectangular, experimental research is required to investigate the CHF for complicated geometries.

For this reason, prediction of CHF by numerical simulation is very attractive, and several studies tried to predict CHF such as [1-2]. This paper reports the result of an investigation of CHF in a vertical channel with CFD. In addition, this study presents numerical simulation results for oscillating vertical pipes.

2. Mathematical and Physical Models

2.1 Wall Boiling Model

Subcooled wall boiling model plays a crucial role in predicting CHF. We used an improved boiling model based on RPI model [3]. The total wall heat flux (q''_w) is combined with heat flux transferring to liquid and heat flux transferring to vapor (q''_G). Heat flux to liquid phase is divided into three components, convective heat flux (q''_C), evaporation heat flux (q''_E), and the quenching heat flux (q''_Q). The total heat flux can be expressed as,

$$q''_w = f(\alpha_l)(q''_C + q''_Q + q''_E) + (1 - f(\alpha_l))q''_G, \quad (1)$$

where $f(\alpha_l)$ is the area fraction of liquid phase, and thus $1 - f(\alpha_l)$ represent the area fraction of vapor phase. This area fraction $f(\alpha_l)$ is based on [4]:

$$f(\alpha_l) = 1 - \max\left[0, \min\left[1, \frac{\alpha_g - 0.9}{0.95 - 0.9}\right]\right]. \quad (2)$$

The four heat fluxes are

$$q''_C = h_l(T_w - T_l)(1 - A_b), \quad (3)$$

$$q''_E = V_d N_w \rho_g h_g f, \quad (4)$$

$$q''_Q = 2\sqrt{k_l \rho_l c_{p,l} f / \pi}(T_w - T_l), \quad (5)$$

$$q''_G = h_g(T_w - T_g), \quad (6)$$

where h_l and h_g stand for the turbulent heat transfer coefficients of liquid and vapor, respectively. T_w, T_g and T_l denote the temperatures of heated wall, vapor and liquid, respectively. A_b is the proportion of heated wall covered by nucleating bubble:

$$A_b = \min\left[1, K\frac{N_w \pi d_{bw}^2}{4}\right]. \quad (7)$$

d_{bw} is the bubble departure diameter based on [5], expressed as

$$d_{bw} = \min\left[0.0006\exp(-\Delta T_{sub} / 45), 0.0014\right]. \quad (8)$$

K is an empirical constant from [6]:

$$K = 4.8\exp\left(\frac{\rho_l c_{p,l}(T_w - T_l)}{80\rho_g L}\right), \quad (9)$$

where L is the latent heat. N_w is the nucleate site density, based on [7]:

$$N_w = 210^{1.805}(T_w - T_{sat})^{1.805}. \quad (10)$$

f is the bubble departure frequency from [8]:

$$f = \sqrt{\frac{4g(\rho_l - \rho_g)}{3d_{bw}\rho_l}}, \quad (11)$$

where g is the gravitational acceleration.

2.2 Interfacial Mass Transfer

Let us denote the vapor generation rate near the wall and the condensation rate in the bulk by Γ_w and Γ_i, respectively. The vapor generation rate is calculated by

$$\Gamma_w = \frac{q''_E A_{wall}}{L + c_{p,l}(T_{sat} - T_l)}, \quad (12)$$

where A_{wall} is the face area of the corresponding cell divided by the cell volume. The subcooled condensation rate is computed by

$$\Gamma_i = \frac{h_{sl} A_i (T_{sat} - T_l)}{L + c_{p,l}(T_{sat} - T_l)}, \quad (13)$$

where h_{sl} is the interfacial heat transfer coefficient [9].

2.3 Eulerian momentum equation in the non-inertial frame of reference

Momentum equations must consider the effect of the arbitrary motion of the pipe. Recently, [10-12] derived the two-fluid momentum equations in the non-inertial frame of reference. The gas and liquid momentum equations are given as follows:

$$\frac{\partial}{\partial t}(\alpha_g \rho_g \mathbf{u}_g) + \nabla \cdot (\alpha_g \rho_g \mathbf{u}_g \mathbf{u}_g) = -\alpha_g \nabla p + \nabla \cdot [\alpha_g (\boldsymbol{\tau}_g + \boldsymbol{\tau}_g^{\mathrm{Re}})] + \mathbf{f}_i + \Gamma_w \mathbf{u}_l + \Gamma_i \mathbf{u}_g + \alpha_g \rho_g \mathbf{g}, \quad -\alpha_g \rho_g \ddot{\mathbf{R}} - \alpha_g \rho_g \dot{\boldsymbol{\Omega}} \times \mathbf{r} - 2\alpha_g \rho_g \boldsymbol{\Omega} \times \mathbf{u}_g - \alpha_g \rho_g \boldsymbol{\Omega} \times (\boldsymbol{\Omega} \times \mathbf{r}) \quad (14)$$

$$\frac{\partial}{\partial t}(\alpha_l \rho_l \mathbf{u}_l) + \nabla \cdot (\alpha_l \rho_l \mathbf{u}_l \mathbf{u}_l) = -\alpha_l \nabla p + \nabla \cdot [\alpha_l (\boldsymbol{\tau}_l + \boldsymbol{\tau}_l^{\mathrm{Re}})] - \mathbf{f}_i - \Gamma_w \mathbf{u}_l - \Gamma_i \mathbf{u}_g + \alpha_l \rho_l \mathbf{g}, \quad -\alpha_l \rho_l \ddot{\mathbf{R}} - \alpha_l \rho_l \dot{\boldsymbol{\Omega}} \times \mathbf{r} - 2\alpha_l \rho_l \boldsymbol{\Omega} \times \mathbf{u}_l - \alpha_l \rho_l \boldsymbol{\Omega} \times (\boldsymbol{\Omega} \times \mathbf{r}) \quad (15)$$

where $\boldsymbol{\Omega}$ and $\mathbf{R}$ are the rotational vector and the position vector of the pipe, when viewed from the absolute coordinates.

$\mathbf{f}_i$ is the interfacial momentum transfer acting on the gas phase, which consists of the drag, lift, wall lubrication, turbulent dispersion, and virtual mass forces.

$\boldsymbol{\tau}_g^{\mathrm{Re}}$ and $\boldsymbol{\tau}_l^{\mathrm{Re}}$ are the turbulent Reynolds stress tensors for the gas and liquid phases. The Realizable k-ε turbulence model was used to calculate the Reynolds stresses.

3. Results and discussion

3.1 Stationary pipe

To validate the present model set, experimental CHF research of [13] were simulated. To benchmark cases, 2.5 inner diameter and 200 mm long vertical tube of stainless steel was employed to investigate CHF in subcooled boiling. A 100 mm long section from entrance was set to be an adiabatic section; another 100mm section was set to be heated as a test section. To simplify the simulation, 1/4 of the pipe was selected as the simulation geometry. Figure 1 shows the schematic of the simulation pipe.

Wall heat flux was ascended by step of 0.5 MW/m² to identify the heat flux value of the CHF. Each heat flux step took 300 iterations for convergence, and a plot of the maximum wall temperature with iteration was recorded. The wall temperature was increased gradually until the heat flux reaches the CHF. When DNB occurred, the maximum wall temperature shot up hundreds of Kelvin. Figure 2 shows the maximum wall temperature for each wall heat flux for the case of V7B2UA [13]. In this case, CHF is identified as 45 MW/m^2. Table 1 lists the simulation conditions and the results. A total of nine sets of data were used to validate the model.

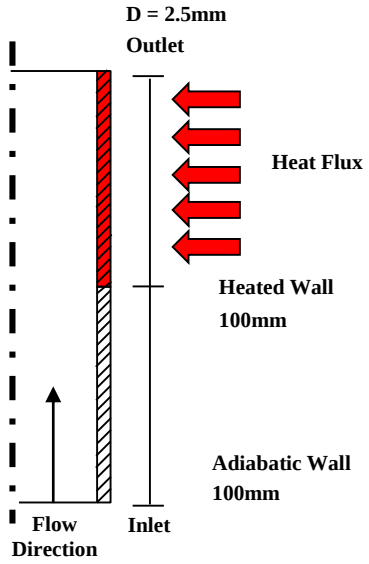

Fig. 1 Schematic of the simulation pipe

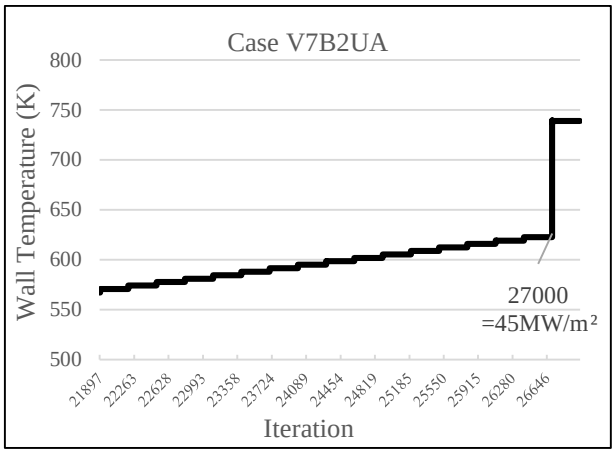

Fig. 2 Maximum wall temperature for each wall heat flux for the case of V7B2UA

Case ID	Conditions			CHF (MW/m²)	
	T_{in} (℃)	G (kg/m2•s)	p (MPa)	Experiment	Prediction
R5U2UA	48.90	29655.4	2.5618	43.37	41.5
R6U2UA	60.24	29695.6	2.5603	47.47	42.5
P3U2UA	70.47	19910.9	2.1019	37.08	31
T3U2UA	30.87	34895.7	2.5807	52.00	56
R4H2UA04	40.23	29819.6	1.4893	55.83	51
V7B2UA	69.82	39323.3	0.8191	43.29	45
R4H2UA02	40.29	29816.9	1.4644	50.72	46.5
V3U2UA01	30.30	39989.6	2.5979	60.57	63
M3U2UA	30.28	20079.4	2.5639	38.27	34

Table. 1 Simulation conditions and results

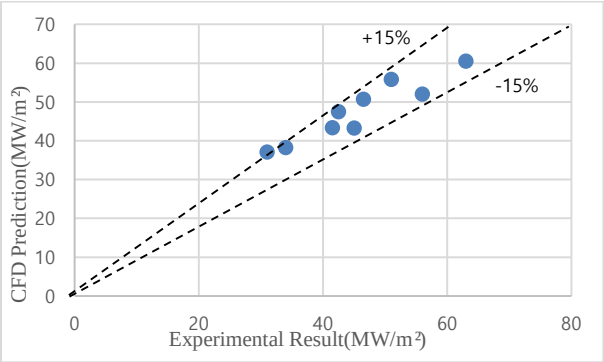

Fig. 3 Comparison of CHF between CFD prediction and experimental result

Figure 3 compares the CHF between CFD prediction and experimental result. The calculated results appear reasonable with deviations less than ±15%. The mean absolute relative error of the calculated CHF data is 8.33%. This excellent result confirms the validity of the present model set for predicting critical heat flux by numerical simulation

3.2 Oscillating pipe

At present, we are performing numerical simulations for critical heat flux in an oscillating pipe [13]. Preliminary results will be presented at the conference.

5. Conclusions

In this study, numerical solution with improved RPI model was employed to investigate the CHF in a vertical pipe. Most of the deviations of calculated CHF from experimental data were below 15%, and the average of absolute relative error was 8.33%. This result agreed quite well with experimental data. Thus, the present boiling model has enough potential to be applied to oscillating pipe cases.

ACKNOWLEDGEMENT

This work was supported by the National Research Foundation of Korea(NRF) grant funded by the Ministry of Science, ICT & Future Planning (No. NRF-2016M2B2A9A02944972)

REFERENCES

[1] Zhang, Rui, et al., Prediction of CHF in vertical heated tubes based on CFD methodology., Progress in Nuclear Energy Vol.78 pp.196-200, Elsevier, 2015
[2] Pezo, Milada, and Vladimir Stevanovic, Numerical prediction of critical heat flux in pool boiling with the two-fluid model., International Journal of Heat and Mass Transfer Vol.54 No.15-16 pp.3296-3303, Elsevier, 2011
[3] Kurul, N. On the modeling of multidimensional effects in boiling channels., ANS. Proc. National Heat Transfer Con. Minneapolis, Minnesota, USA, 1991.
[4] Ioilev, Andrey, et al., Advances in the modeling of cladding heat transfer and critical heat flux in boiling water reactor fuel assemblies, Proc. 12th International Topical Meeting on Nuclear Reactor Thermal Hydraulics (NURETH-12), Pittsburgh, Pennsylvania, USA, 2007.
[5] Tolubinsky, V. I., and D. M. Kostanchuk., Vapour bubbles growth rate and heat transfer intensity at subcooled water boiling, International Heat Transfer Conference 4. Vol.23, Begel House Inc., 1970.
[6] Del Valle, Victor H., and D. B. R. Kenning, Subcooled flow boiling at high heat flux., International Journal of Heat and Mass Transfer Vol.28 No.10 pp.1907-1920, 1985
[7] Lemmert, M., and J. M. Chawla, Influence of flow velocity on surface boiling heat transfer coefficient., Heat Transfer in Boiling Vol.237 pp.247, 1977
[8] Cole, Robert, A photographic study of pool boiling in the region of the critical heat flux, AIChE Journal Vol.6 No.4 pp.533-538, 1960
[9] Ranz, W. E., and W. R_ Marshall, Evaporation from drops, Chem. Eng. Prog Vol.48 No.3 pp.141-146, 1952
[10]B. J. Kim and K. D. Kim, Two-fluid equations for a nuclear system with arbitrary motions, Transactions of the Korean Nuclear Society Autumn Meeting, Gyeongju, Korea, October 27-28, 2016.
[11] M. H. Kim and B. J. Kim, Demonstration of numerical simulation of multi-dimensional two-phase flow for a marine reactor, Transactions of the Korean Nuclear Society Autumn Meeting, Gyeongju, Korea, October 26-27, 2017.
[12] B. J. Kim, M. H. Kim, S. W. Lee, and K. D. Kim*, Two-fluid equations for two-phase flows in moving systems, Submitted, 2018.
[13] Celata, G. P., M. Cumo, and A. Mariani, Burnout in highly subcooled water flow boiling in small diameter tubes, International Journal of Heat and Mass Transfer Vol.36 No.5 pp.1269-1285, Elsevier, 1993